

# Attenuation of Harmonics Utilizing new Control Strategies for the SVC in Brazilian Power System

I. R. Machado, C. Couto, E. L. van Emmerik, M. Aredes

Universidade Federal do Rio de Janeiro – COPPE / UFRJ

Laboratório de Eletrônica de Potência e Média Tensão – LEMT

Caixa Postal: 68504, CEP: 21949-900

[isaac@coe.ufrj.br](mailto:isaac@coe.ufrj.br), [christiana@lemt.ufrj.br](mailto:christiana@lemt.ufrj.br), [emmerik@lemt.ufrj.br](mailto:emmerik@lemt.ufrj.br), [aredes@lemt.ufrj.br](mailto:aredes@lemt.ufrj.br).

**Abstract** – Due to the high level of compensation with parallel reactors and series capacitors at the 500 kV transmission lines that interconnect the South and North regions of Brazil (from Serra da Mesa to Imperatriz substation), and the long distance compensation with parallel reactors at the South-East/North-East interconnection, harmonic resonances around 120 Hz and others occur in this region. This concerns directly to the SVC of Bom Jesus da Lapa (BJL), since this Power Electronic Compensator is capable of responding in this frequency range. This paper shows the capability of the SVC to attenuate harmonic resonances.

**Keywords** – Attenuation, Frequency Dependent Line Models, Harmonic propagation, Reactive Power, SVC, Transmission System.

## I. INTRODUCTION

The main motivation for the study presented in this paper is the harmonic propagation in the vicinity of BJL. Due to high level 5th harmonic propagations in this region, one of the filters of the SVC has been damaged because of overload.

To simulate this event, the transmission grid in voltage levels of 500, 230 and 69 kV near the Substation BJL where modeled in PSCAD/EMTDC [6]-[10]. The SVC and its actual control system were implemented as well in this simulation program. A new control scheme to avoid overloading of the 5th harmonic filter was developed.

Figure 1 shows the modeled Transmission Lines with PI models and Frequency Dependent Phase Models. Three dynamic equivalents can be observed, representing the regions North, Southeast and Northeast [1]. A 5th harmonic current source was inserted at the Substation Juazeiro 69 kV to verify the harmonic propagation and its effects on the filters. This substation was chosen due to resonance studies in the frequency domain and presence of industry fed by this substation.

The SVC of BJL substation (250 Mvar) [8]-[12], as shown in Figure 1, can be utilized to collaborate with the mitigation of electromechanical oscillations [13]-[16] as for the attenuation of harmonic resonance and propagation at the system. In fact, the control system of the SVC of Bom Jesus da Lapa has an input for an additional signal, which was inhibited, and can be utilized for other purposes than the basic voltage control function of the South-East/North-East interconnection.

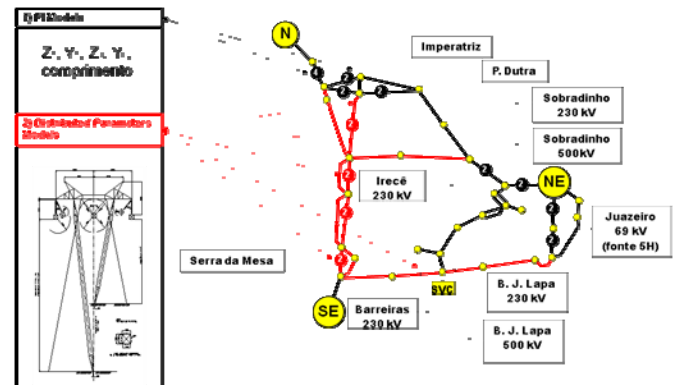


Fig. 1. Interconnected System North / North-East / South-East Modeled.

The following section shows in more detail the modeling of the transmission lines and SVC of BJL. Section III presents the control system of the SVC and Section IV shows the validation through simulation results.

## II. LINES TRANSMISSIONS MODELS

This section contains the representation of the transmission lines (models with concentrated and distributed parameters) and the process of implementation in PSCAD/EMTDC. Figure 2 shows the entire implemented model, constituted of various modules and sub-modules.

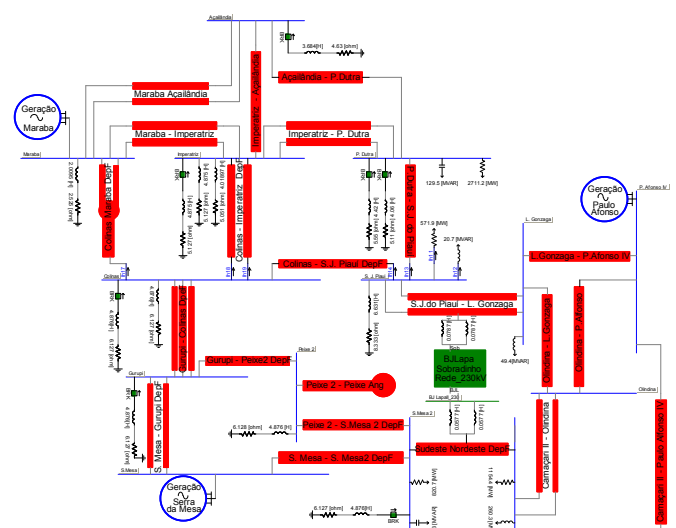


Fig. 2. The System in PSCAD/EMTDC.

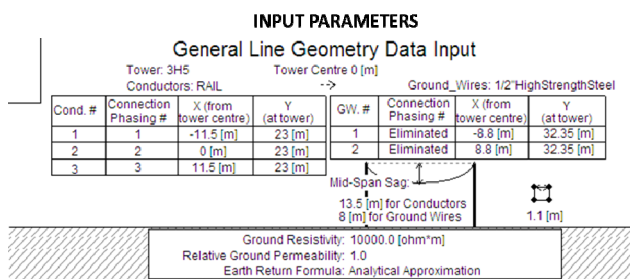
### A. Distributed Parameters Models (Frequency Dependent)

The procedure to model the sections in distributed parameters is basically filling in the table shown in Fig.3. The tower geometry data, phase conductor and ground wire distribution, sag, conductors' constructive characteristics and soil properties are all inserted by the user and the values of the positive, negative and zero sequences are calculated. The line transposition is made at 1/6, 1/2 and 5/6 of their total length.

The sequence parameters are influenced by the different tower geometries. For example, the positive sequence reactance is a parameter influenced mainly by the bundle geometry and the separation between phases, as the positive sequence resistance is affected by the cable constructive characteristics.

Fig. 3 shows data of the analyzed tower geometry for the section in which SVC is situated (Northwest/Southwest). The respective values of the positive, negative and zero sequences obtained from PSCAD/EMTDC input data are compared with the values of the concessionaire responsible for the line transmission operation. One can observe that the parameters from the input data ("Real Parameters") and the calculated values ("Simulated Results") shown in Fig. 3. are close.

REAL LINE GEOMETRY									
METRIC									
C ESL - 3/8"EAR + OPGW									
C 4x954MCM EXPANDIDO									
1.375	.0718	4	2.959	-11.5	23.00	9.5	110.	45.	
2.375	.0718	4	2.959	0.	23.00	9.5	110.	45.	
3.375	.0718	4	2.959	11.5	23.00	9.5	110.	45.	
0.170	0.430	4	1.540	-8.80	32.35	23.35			
0.5	4.188	4	.914	8.80	32.35	23.35			



### REAL PARAMETERS(Ohms/km)

Sequence	Resistance ohm/km	Reactance ohm/km	Susceptance mho/km
Zero	2.80063E-01	9.79454E-01	3.96425E-06
Positive	1.87812E-02	2.72523E-01	6.21468E-06

### SIMULATED PARAMETERS(Ohms/km)

Sequence Impedance(ohms)		
	R	X
POS	0.0186912022	0.27229301
NEG	0.0186912022	0.27229301
ZERO	0.272742447	0.902184497

Sequence Admittance(mhos)		
	G	B
POS	1.0e-008	6.21232899e-006
NEG	1.0e-008	6.21232899e-006
ZERO	1.0e-008	3.95684709e-006

Fig. 3. Distributed parameter modeling and generated sequence parameters.

### B. Concentrated Parameters Models (PI Models)

The PI model is constituted by concentrated parameters of resistance, inductance and capacitance obtained from the data inserted by the user (Fig. 4). The data is provided in sequence components. Therefore, the circuit elements are presented in matrix format taking into consideration the inductive and capacitive coupling between the phases.

All sequence component data of the transmission lines, bar reactors, line reactors and series capacitor compensation were obtained from ONS (National System Operator) and software provided by CEPEL (Centro de Pesquisa de Energia Elétrica). Fig. 4. shows the data entry tables for the PSCAD/EMTDC PI model for the filling in of the positive and zero sequences (in  $\Omega/m$  and S.m) and line length.

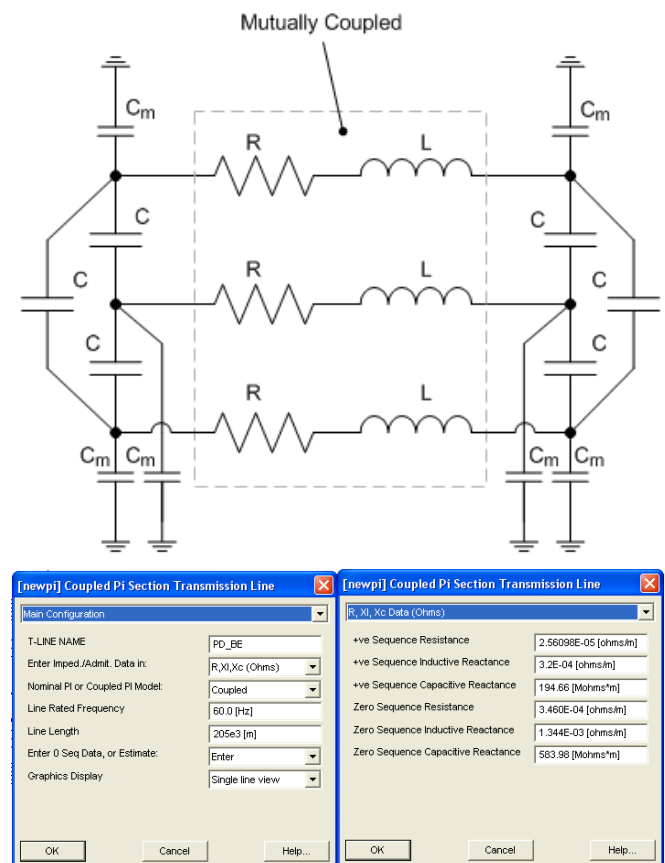


Fig. 4. Concentrated parameter modeling.

## III. SVC MODEL

### A. Power Circuit

The BJL's SVC (Fig. 5) contains two branches of Thyristor Controlled Reactors (TCR), one branch of Thyristor Switched Capacitors (TSC) and two tuned filters (F1 and F2) connected through a breaker. Using two TCR and one TSC branch enables a degraded operation mode in case any switch in one of the branches is out of service and sustain an effective control with any TCR out of service.

Table I provides a resumed overview of the reactive power of the different branches for a capacitive and inductive mode operation in 1.0 p.u. at the high-voltage side, at nominal frequency and nominal component values (Table II).

The sum of the reactive power of the capacitive branches ( $194.1 + 91.0 = 285.1$  MVAR) is reduced to 250.1 MVAR at the high voltage side due to transformer inductance. The TCRs and filters sum ( $267,0 - 51,8 = 215,2$  MVAR) with an inductive operation is elevated to 250,2 MVAR due to the transformer.

The reactive power values for the SVC ( $Q_{SVC}$ ), as shown in Table I, result in an output reactive power of 250 MVAR capacitive and 250 MVAR inductive for nominal voltage. This nominal output power is continuously available for a voltage of 500 kV + 5%.

The filters are tuned for 5th (F1) and 7th (F2) harmonics and connected in non-grounded Wye, and the TSC are tuned in 240 Hz and connected in Delta. Table II shows the nominal values of the SVC's components.

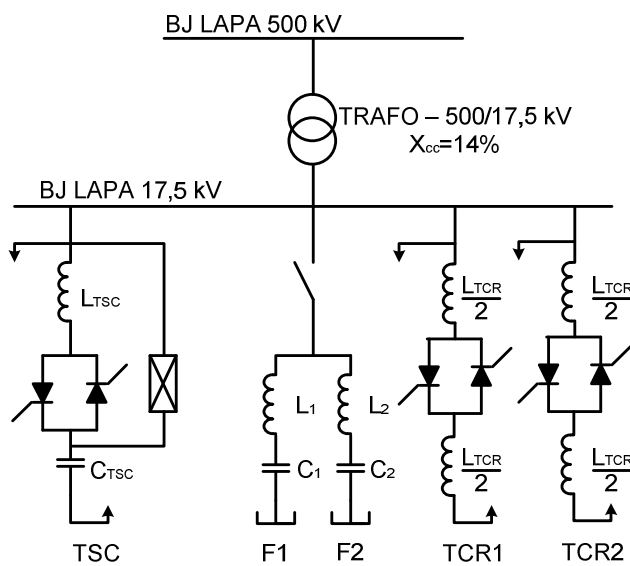


Fig. 5. SVC - Power circuit.

TABLE I  
SVC operation range

	$Q_{SVC}$ [MVA]	$Q_{TCR}$ [MVA]	$Q_{TSC}$ [MVA]	$Q_{FILTER}$ [MVA]
Capacitive	250,4	0	194	91,3
Inductive	250	267,5	0	51,9

TABLE II  
Nominal parameters

	Capacitance or Inductance	Nominal Current (A)
$L_1$	1,4 mH	1000
$L_2$	0,38 mH	1770
$C_1$	210 $\mu$ F	1000
$C_2$	380 $\mu$ F	1770
$L_{TSC}$	1,1 mH	3406
$C_{TSC}$	404 $\mu$ F	3406
$L_{TCR}$	13,5 mH	3400

### B. Control Circuit

The SVC's control scheme is shown in a simplified way in Fig. 6. The control system consists basically in the comparison between a reference voltage,  $V_{ref}$ , and a measured value at the 500 kV bar,  $V_{act}$ . The error is made zero through a PI giving at its output the needed susceptance. The reference voltage can vary from 0.95 to 1.05pu in 5kV

steps. The slope can vary from 0 to 10% and is based on the static compensator's reactive power. The susceptance allocator defines the operation point of each device (TCR1, TCR2 e TSC) based on the susceptance value.

The currents in the filters are constantly monitored and the data has priority over the determination of the thyristors' fire angles. One can observe that as these angles get closer to  $110^\circ$  and  $130^\circ$  they have more harmonic pollution. Therefore, the circuit control avoids these fire angles when it will overload the filter.

When the current in the 5 harmonic filter exceeds its nominal value the fire angle of one TCR is diverted towards  $90^\circ$ ,  $130^\circ$  or  $180^\circ$  (angles that provide less 5 harmonic content). The second TCR's angle can also be modified in case a change of the first TCR's fire angle doesn't decrease the current sufficiently. In case of an exceptional high pollution coming from the grid the breaker still have to be activated to protect the filters.

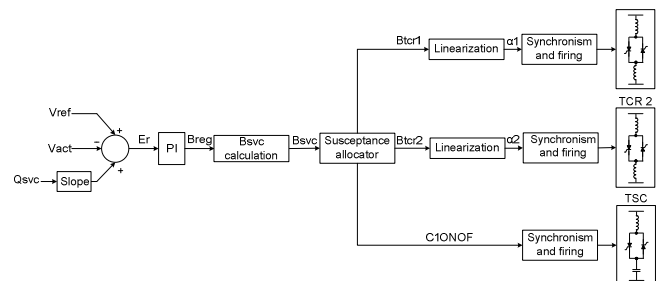


Fig. 6. SVC - Control strategy.

## IV. SIMULATIONS

### A. Case without TSC

The simulation results are shown in case of the SVC operating in inductive mode. At this operation point the TCR1 is with a  $110^\circ$  fire angle and TCR2 with a  $90^\circ$  one. The TSC is not operative. A polluting current source injects the 5<sup>th</sup> harmonic in the Juazeiro 69 kV bar. The propagation of the 5<sup>th</sup> harmonic current makes the filter operate in a 1.12 kA current, therefore, over the nominal current (1 kA).

The increase of the TCR1 fire angle to  $130^\circ$  occurs instantly at 0.5 seconds. The 5<sup>th</sup> harmonic current produced by the TCR1 flows from a max to a minimum value according to the simulated graphic shown in Fig. 7. The reduction in the 5th harmonic current component is shown in Fig. 11. A slight increase in the fundamental current is observed as well (Fig. 10), since the new SVC operation point is changed from inductive to capacitive (Fig. 8) resulting in a higher voltage at the 500 kV bar.

This alteration of the RMS value of the voltage in the 500 kV bar is from 1.04 p.u., at 0.5 s, to 1.06 p.u. at 0.6 s (Fig. 9). The TCR1 fire angle change resulted in a SVC inductive operation point change from -40 MVAR to 30 MVAR (Fig. 8). All the simulation results are shown after 0.4 s when the system has reached a steady state. Changing the fire angle of one TCR reduced the current in the 5<sup>th</sup> harmonic filter to a value below the maximum allowed (Fig. 12).

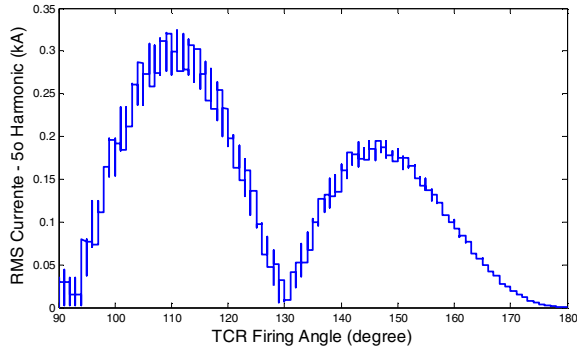


Fig. 7. 5<sup>o</sup> Harmonic current in a TCR branch.

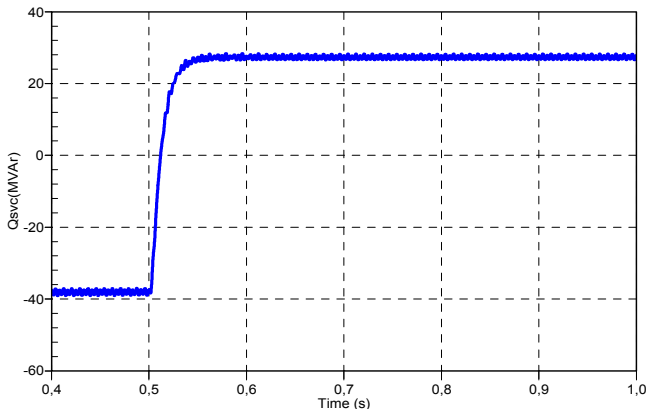


Fig. 8. SVC reactive power (without TSC).

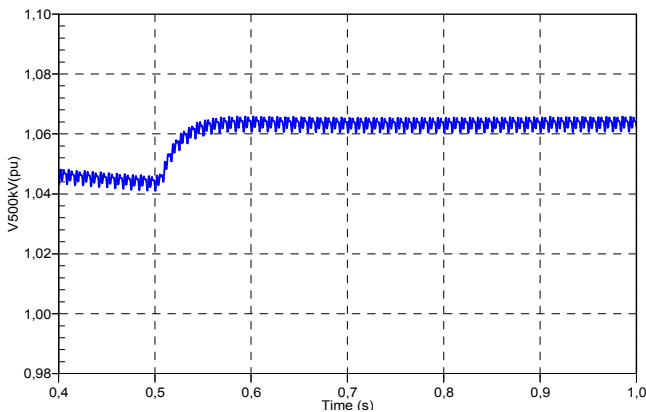


Fig. 9. Bom Jesus da Lapa RMS voltage (without TSC).

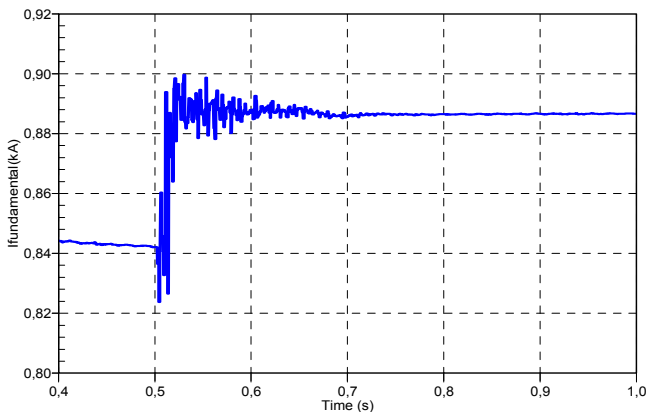


Fig. 10. Fundamental current in the 5th harmonic filter (without TSC).

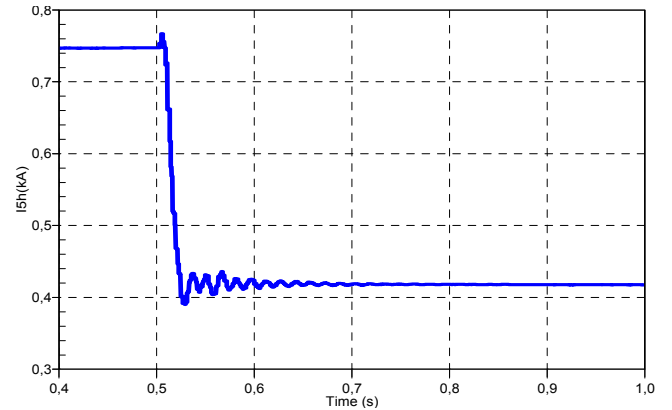


Fig. 11. 5th harmonic current in the 5th harmonic filter (without TSC).

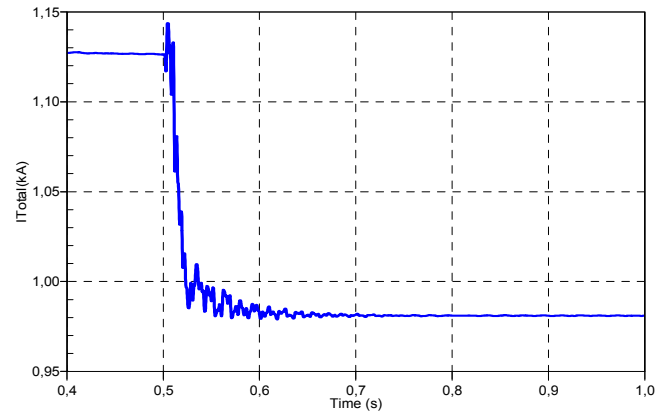


Fig. 12. Total current in the 5th harmonic filter (without TSC).

### B. Case with TSC

The simulation results are shown in case of the SVC operating in capacitive mode. At this operation point the TCR2 firing signals are blocked and TCR1 fire angle changes, in 0.5 s, from 110° to 130°. The TSC is operating. A polluting current source injects the 5<sup>th</sup> harmonic in the Juazeiro 69 kV bar. The propagation of the 5<sup>th</sup> harmonic current makes the filter operate in a 1.05 kA current, therefore, over the nominal current (1 kA).

When the fire angle is changed, the TCR operation resulted in a operation point change from 129 MVar to 210 MVar (capacitive) (Fig. 13). This modifies the RMS value of the voltage in the 500 kV bar from 1.03 p.u., at 0.5 s, to 1.05 p.u (Fig. 14). Therefore, one expects that the fundamental current increases. One can observe this change from 0.9 to 0.95 (kA) in Fig. 15. Also, the 5<sup>th</sup> harmonic component is reduced from 0.52 to 0.26 kA as shown in Fig. 16.

The increase in the fundamental component is more than compensated by the decrease in the 5<sup>th</sup> harmonic current resulting in a lower total current in the filter (Fig. 17). All the simulation results are shown after 0.4 s when the system has reached a steady state. Modifying the TCR1 fire angle, with the TSC operating, reduced the current in the 5<sup>th</sup> harmonic filter to a value below the maximum allowed.

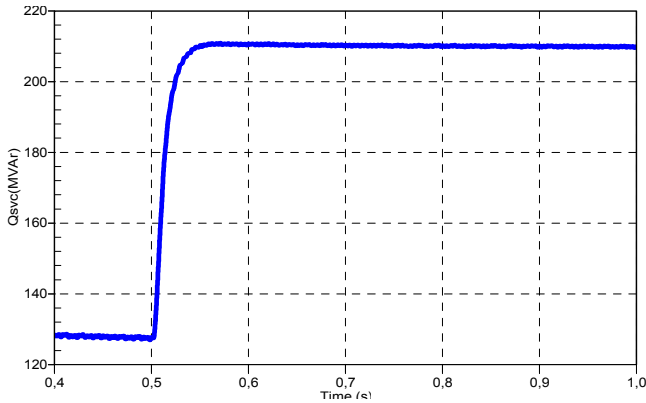


Fig. 13. SVC reactive power.  
(With TSC and instant 20° angle change)

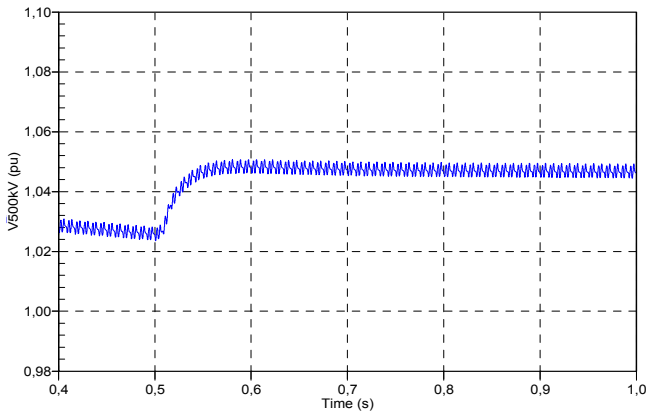


Fig. 14. Bom Jesus da Lapa RMS Voltage  
(With TSC and instant 20° angle change)

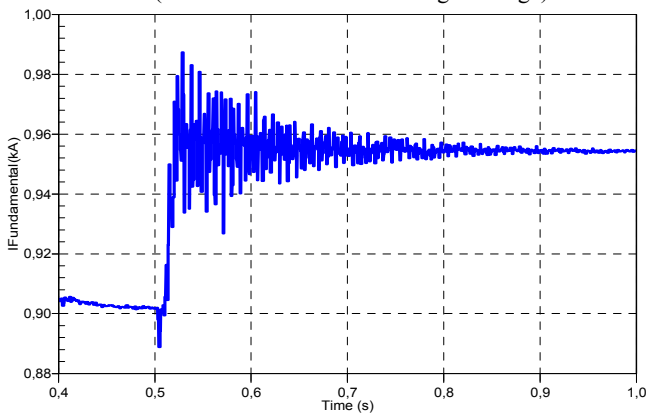


Fig. 15. Fundamental current in the 5<sup>th</sup> harmonic filter.  
(With TSC and instant 20° angle change)

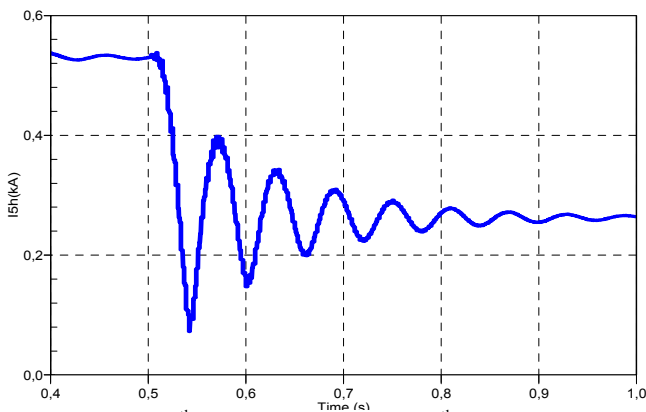


Fig. 16. 5<sup>th</sup> harmonic current in the 5<sup>th</sup> harmonic filter  
(With TSC and instant 20° angle change)

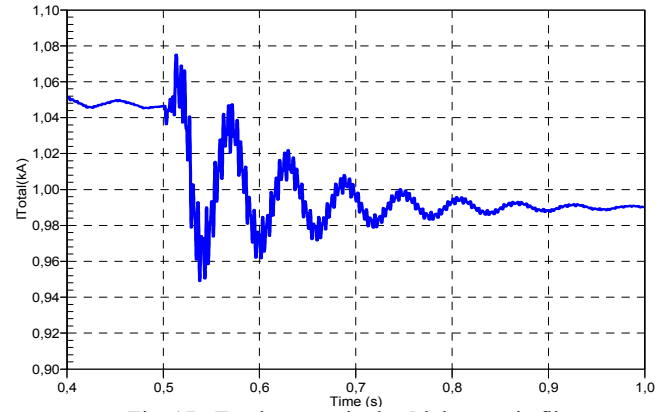


Fig. 17. Total current in the 5<sup>th</sup> harmonic filter.  
(With TSC and instant 20° angle change)

One can observe expressive oscillations at Fig. 15 to Fig. 17 in the current components. This happens due to the unusual fire angle change step. When there is a TCR1 fire angle ramped increase, during 0.1 s, from 110° to 130°, the results maintain the same behavior, although the expressive oscillations in the currents components are significantly smoothed as can be observed at Fig. 18 to Fig. 22.

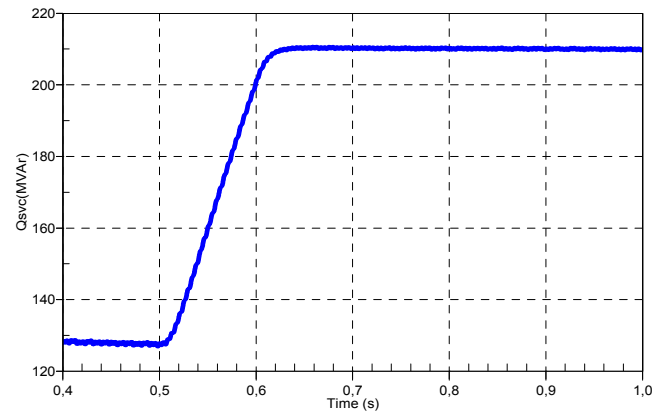


Fig. 18. SVC reactive power.  
(With TSC and 20° ramped angle)

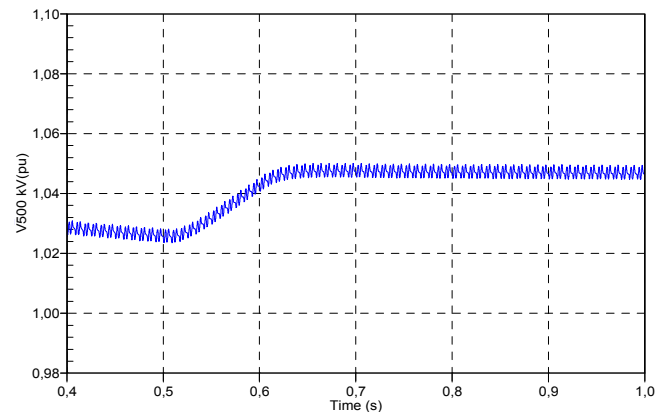


Fig. 19. Bom Jesus da Lapa RMS Voltage  
(With TSC and 20° ramped angle)

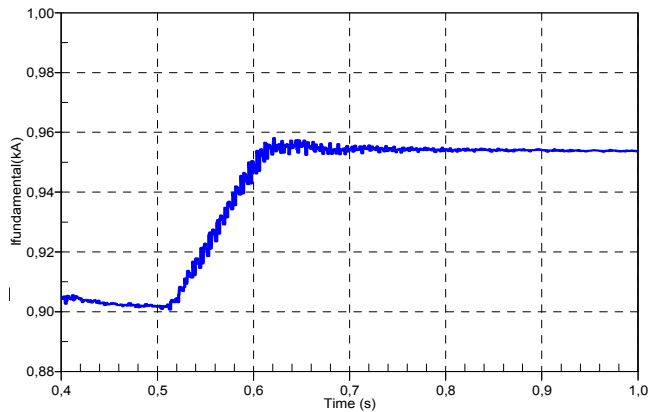


Fig 20. Fundamental current in the 5<sup>th</sup> harmonic filter.  
(With TSC and 20° ramped angle)

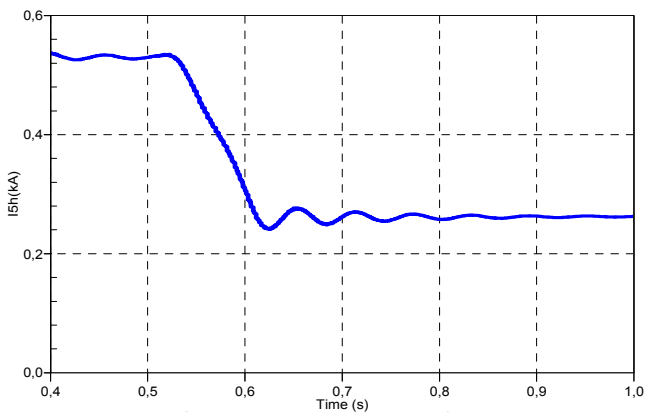


Fig.21.5<sup>th</sup> harmonic current in the 5<sup>th</sup> harmonic filter  
(With TSC and 20° ramped angle)

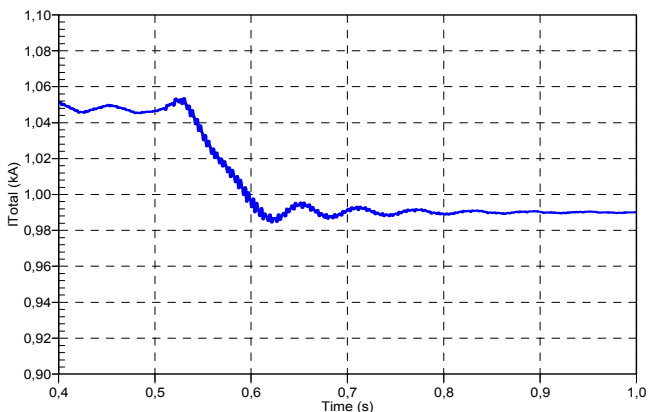


Fig. 22. Total current in the 5<sup>th</sup> harmonic filter.  
(With TSC and 20° ramped angle)

## V. CONCLUSION

This article has shown an additional control strategy for the SVC. The method consists of changing the TCR's fire angle in case of overload. The SVC's harmonic production as a function of the fire angle as shown in Fig. 7 is utilized to diminish the harmonic content when necessary, maintaining at the same time the voltage at the BJL bus within acceptable operation limits. Such methodology intends to reduce the 5<sup>th</sup> harmonic currents when overloading occurs avoiding that the SVC has to be taken out-of-service.

The simulation results have shown satisfactory results in relation to the filter loading (Figs. 12 and 17).

## ACKNOWLEDGEMENT

The authors would like to express gratitude for the financial support of TAESA, CAPES and CNPq.

## REFERENCES

- [1] Gama, C. - Brazilian North-South Interconnection control-application and operating experience with a TCSC - IEEE Summer Power Meeting, 1999.
- [2] Gama, C.; Tenorio, R. - Improvements for power systems performance: modeling, analysis and benefits of TCSC, IEEE Winter Power Meeting, 2000.
- [3] Gomes, P.; dos Santos, M. G.; Aquino, A. F. C; Barbosa, A. B.; de Oliveira, V. R. - Experiência Brasileira com a Utilização de TCSC em circuitos paralelos – ERIAC 2005, Paraguai, 2005.
- [4] [http://www.ons.org.br/operacao/diagramas\\_impedancias.aspx](http://www.ons.org.br/operacao/diagramas_impedancias.aspx)
- [5] [http://www.ons.org.br/plano\\_ampliacao/plano\\_ampliacao.aspx](http://www.ons.org.br/plano_ampliacao/plano_ampliacao.aspx)
- [6] CEPEL, Centro de Pesquisas de Energia Elétrica "ANAREDE, Programa de Análise de Redes". DSE, Departamento de Sistemas Elétricos.
- [7] CEPEL, Centro de Pesquisas de Energia Elétrica "ANAT0, Programa de Análise de Redes em t0+". DSE, Departamento de Sistemas Elétricos.
- [8] Erickson, R.W., Fundamentals of Power Electronics, Chapman and Hall, 1997
- [9] Hingorani, N.G., Gyugi L., Understanding FACTS, Wiley IEEE Press, 1999
- [10] Kundur P., Power System Stability and Control. New York: McGraw-Hill Inc, 1994
- [11] Acha E., Fuerte-Esquivel C. R., Ambriz-Perez H., Angeles Camacho C., FACTS Modelling and Simulation in Power Networks, John Wiley & Sons, 2004
- [12] Francois J., Datta S., SVC protection and control basics, 58th Annual Conference for Protective Relay Engineers, 2005
- [13] Luo A., Z. Shuai, et al, Combined System for Harmonic Suppression and Reactive Power Compensation, IEEE Transactions on Industrial Electronics, 2009
- [14] Gelen, A., Yalcinoz, T., Analysis of TSR-based SVC for a Three-Phase System with Static and Dynamic Loads, International Conference on Electrical Engineering, 2007
- [15] Zhu J., Cheung K., Hwang, D.; Sadjadpour, A. Voltage Profile Evaluation of Power Systems with coordinated SVC devices, Power Systems Conference and Exposition, 2009
- [16] Tenti P. Trombetti, D., Tedeschi E., Mattavelli P., Compensation of Load Unbalance, Reactive Power and Harmonic distortion by cooperative operation of distributed compensators, 13th European Conference on Power Electronics and Applications, 2009.